THE JOURNAL OF PHYSICAL CHEMISTRY C



C: Energy Conversion and Storage; Energy and Charge Transport

# Complete Characterization of Thermoelectric Materials by Impedance Spectroscopy

Braulio Beltrán-Pitarch, Jesús Prado-Gonjal, Anthony V. Powell, Fernando Martinez-Julian, and Jorge García-Cañadas

*J. Phys. Chem. C*, **Just Accepted Manuscript** • DOI: 10.1021/acs.jpcc.9b02131 • Publication Date (Web): 01 May 2019

# Complete Characterization of Thermoelectric Materials by Impedance Spectroscopy

Braulio Beltrán-Pitarch[1], Jesús Prado-Gonjal[2], Anthony V. Powell[2], Fernando Martínez-Julián[3], Jorge García-Cañadas[1,*]

[1]*Department of Industrial Systems Engineering and Design, Universitat Jaume I, Campus del Riu Sec, 12071 Castellón, Spain*

[2]*Department of Chemistry, University of Reading, RG6 6AD, Reading, UK*

[3]*Instituto Universitario de Tecnología Cerámica, Universitat Jaume I, Campus del Riu Sec, 12071 Castellón, Spain*

[*]*e-mail: garciaj@uji.es*

**ABSTRACT**

Thermoelectric materials can directly convert waste heat into electricity. Due to the vast amount of energy available as waste heat in our society, these materials could contribute to reduce our dependence on fossil fuels and their associated environmental problems. However, the heat to electricity conversion efficiency of thermoelectric materials is still a limiting factor, and extensive efforts are being undertaken to improve their performance. The search for more efficient materials is focused on the optimization of three properties (Seebeck coefficient, electrical resistivity, and thermal conductivity). Typically, these are determined as function of temperature through independent measurements on two or more instruments, making thermoelectric characterization tedious and time consuming, which complicates the attainment of a more efficient heat to electricity energy conversion. Here, it is demonstrated for the first time that a complete thermoelectric characterization of a material may be achieved from a single electrical measurement performed on one instrument only, by employing the impedance spectroscopy method. A skutterudite sample is used for the demonstration, which is sandwiched between two stainless steel contacts in a four-probe arrangement and their properties are determined from 50 to 250 ºC. This new approach shows good precision and agrees with characterization of the same sample performed with commercial equipment, illustrating the power of the technique to facilitate the rapid and efficient evaluation of thermoelectric materials.

## 1. INTRODUCTION

Nowadays, more than 60% of the global power is lost as waste heat, which represents ≈15 TW. A 10% recovery of this energy will exceed the summation of most current renewable energy sources (solar, wind, geothermal, and hydro energy).[1] Thermoelectric (TE) materials can directly convert waste heat into electricity. Due to this, they have interest in applications such as automobiles and industries, where they can generate energy from the waste heat released by exhaust gases and reduce $CO_2$ emissions.[2] They can also convert solar warmth into electricity when integrated in solar thermoelectric generators.[3] In addition, they are also potentially able to power wearable electronics and sensors using environmental heat or from human bodies, being a top candidate for self-powering sensors from the internet of things, empowering the elimination of batteries, which are toxic and subjected to frequent recharging and replacement.[4] An efficient heat to electricity energy conversion from these applications would help to reduce our dependence on fossil fuels and their associated environmental problems.

However, the efficiency of current TE materials is still limited. The search for more efficient materials is guided by the optimization of three properties, the electrical conductivity $\sigma$, the Seebeck coefficient $S$, and the thermal conductivity $\lambda$ (which is the addition of the lattice thermal conductivity and the electronic thermal conductivity). These define a dimensionless figure of merit $zT=\sigma S^2 T/\lambda$, $T$ is the absolute temperature, which is related to the materials efficiency.[5] $zT$ is typically obtained by the independent measurement as a function of temperature of $\sigma$, $S$, and $\lambda$. This usually requires at least two different instruments. $S$ and $\sigma$ can be measured using a single apparatus, while the most frequently used method to determine $\lambda$ is the laser flash technique, which provides the thermal diffusivity $\alpha$. Thus, knowledge of the specific heat $C_p$ and the mass density $d$ is required, since $\lambda=\alpha dCp$.[6] The measurement of the specific heat requires an additional measurement, performed either by using the same laser flash equipment or another instrument. For the mass density, an Archimedes balance is frequently employed. The significant number of instruments required, each with their own sources of error, and the large number of measurements to be performed, makes the task of completely characterization of TE materials quite tedious and time consuming. In addition, much of the required equipment is quite expensive, and hence not always readily accessible to all researchers. All these disadvantages entail significant obstacles in the search for better TE materials, eventually affecting the attainment of a more efficient heat to electricity energy conversion.

Several techniques have been developed which allow the complete characterization of TE materials.[7–11] Here a new method is proposed, which unlike the previously reported techniques does not require two identical samples nor the creation of a temperature gradient across the sample, the measurement of which can introduce significant uncertainty.[12] In addition, the determination of the TE properties does not require a series of measurements, as all properties can be extracted from a single measurement. To our knowledge, this is the first time that all these advantages are offered by a measurement technique. The method is based on the measurement of the impedance signal of a TE sample that is sandwiched by a material of known thermal conductivity. Although the application of impedance spectroscopy to thermoelectricity dates back from the 2000s,[13,14] this approach was proposed by us in 2014,[15] and it has only been demonstrated to date in TE modules.[16–18] Here the approach is applied to a skutterudite material, for which complete TE characterization is achieved up to 250 ºC (although with some deviations in $\sigma$ at the higher temperatures). The results are compared with the values of the TE properties determined using commercially available equipment, and the random and systematic errors are calculated. The fact that the new method is based on impedance spectroscopy introduces additional advantages, since it is a widely used technique in many fields of research (solar cells,[19,20] fuel cells,[21] supercapacitors,[22] corrosion,[23] electroceramics,[24] etc.). For this reason, highly reliable impedance equipment exists in the market and can be found in many research institutions, which makes the method more accessible.

## 2. EXPERIMENTAL SETUP

The setup employed for the complete characterization of the skutterudite sample is shown in Fig. 1. It is similar to the setup employed in our previous work to characterize TE materials of known Seebeck coefficient.[25] Unlike the previously reported setup, the TE sample ($CoSb_{2.75}Sn_{0.05}Te_{0.20}$ skutterudite[26] of 1.85 mm x 2.13 mm x 6.95 mm) is here sandwiched by two stainless steel (AISI 304) contacts of the same cross-sectional area and 2 mm thickness. A four-probe arrangement is employed (see inset of Fig. 1), where the current is injected and extracted by two sharpened stainless steel screws and the voltage is measured across the sample by inserting very thin (15 µm diameter, Alfa Aesar) tungsten wires at the junctions. These wires are used instead of the Cu wires employed in our previous study since reactions with the stainless steel were observed for copper at higher temperatures. In order to minimize the electrical and thermal contact resistances, a layer of a liquid metal (GaInSn, Alfa Aesar) is homogeneously spread at the junctions (see inset of Fig. 1).

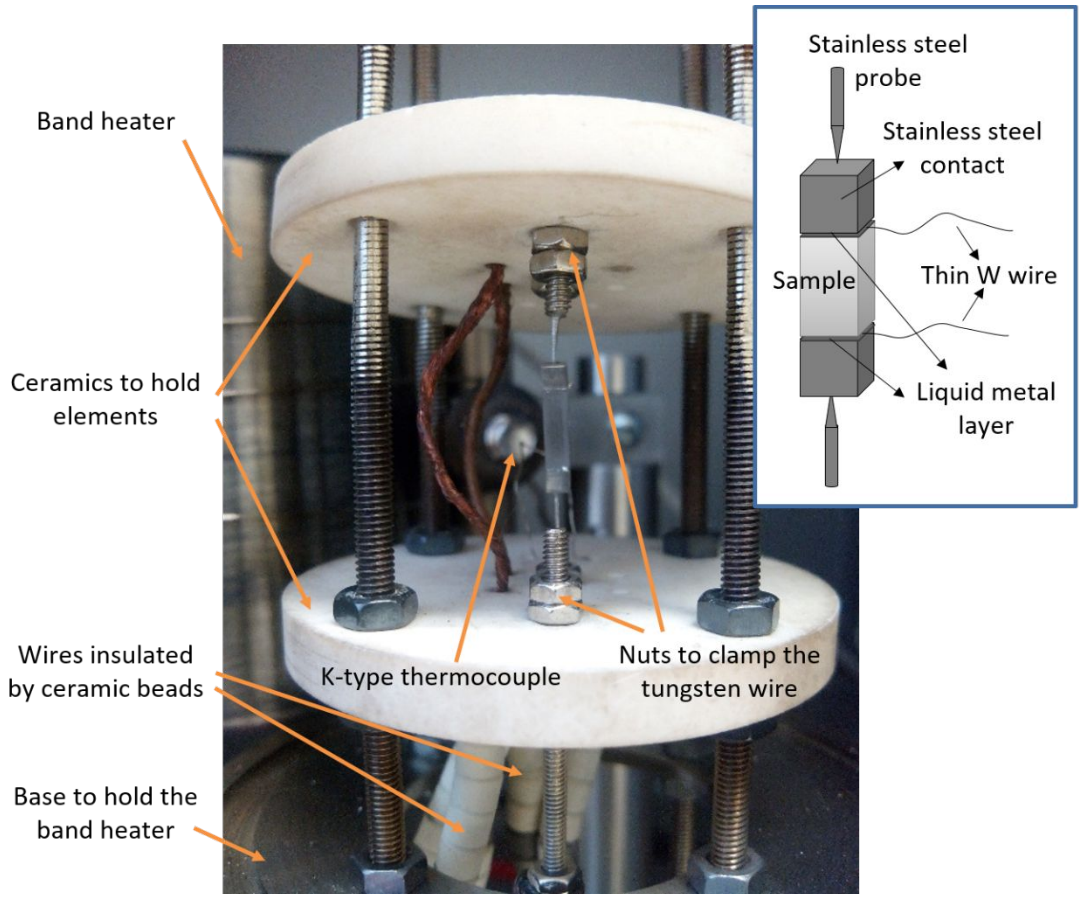


Fig. 1. Photograph of the sample holder employed. A schematic description of how the sample is contacted is provided in the inset.

The two stainless steel screws which drive the current are held by nuts at holed ceramics (Macor, Corning) which provide electrical insulation, as shown in Fig. 1. These screws are connected to thick copper wires insulated by ceramic beads. Stainless steel screws were chosen due to their low thermal conductivity (≈14 $W/K^{-1}m^{-1}$), which reduces heat losses by conduction. They were also sharpened for the same purpose. The very thin tungsten wires that measure the potential difference are clamped at the sample holder by two nuts screwed with stainless steel screws, which are held by the ceramic plates (see Fig. 1). These screws are also connected to thick copper wires insulated by ceramic beads. The bottom holed ceramic disc is fixed at four threaded studs by nuts, while the top ceramic is free to move to be able to allocate samples of different lengths, and additionally provide pressure to the contacts. A stainless steel base is also held by nuts at the studs. This base is used to hold a band heater (Ref.

MB2E2JN1-B12, Watlow) which surrounds the sample holder and is used to provide different ambient temperatures. The ambient temperature is measured by a K-type thermocouple (RS) placed close to the TE sample (see Fig. 1), whose temperature is controlled by a temperature controller (Watlow EZ Zone PM) which powers the heater.

All the impedance measurements were performed inside a stainless-steel vacuum chamber at pressure values $<10^{-4}$ mbar in order to eliminate convection heat losses. In addition, the metallic vacuum chamber also serves as a Faraday cage, which reduces electromagnetic noise during the measurements. The TE sample used in this study was an isotropic n-type skutterudite ($CoSb_{2.75}Sn_{0.05}Te_{0.20}$), which was cut with a diamond saw of 0.3 mm diameter from an original disc shape. A careful and suitable cutting is important to obtain a crack free sample of highly uniform cross-sectional area. The skutterudite sample was characterized using commercial equipment in its disc shape before performing the impedance measurements. A Linseis LSR-3 equipment was used to determine the electrical resistivity and the Seebeck coefficient. For the thermal conductivity a Netzsch LFA 447 laser flash apparatus was employed. The specific heat of the sample was determined using the same equipment via a comparative method using a Pyroceram reference sample. The density of the sample, which is also required for the determination of the thermal conductivity by the laser flash method, was measured using an Archimedes balance.

A PGSTAT30 potentiostat (Metrohm Autolab B.V.) equipped with a FRA2 impedance module and a BOOSTER10A, was used to perform the impedance spectroscopy measurements. The potentiostat was controlled by the Nova 1.11 software. At each temperature the impedance measurement was conducted in 40 logarithmically distributed frequency steps between 5 mHz and 500 Hz. The measurements were performed using a maximum integration time of 10 s and 2 minimum integration cycles. The fitting to the impedance spectra were performed using Zview software. In our previous paper it was discussed the use of the current booster to reduce a systematic jump in the real impedance produced due to a change in the gain of the equipment, which occurs at frequencies around 25 Hz. Although this jump can be significantly reduced if measurements are performed in the largest possible current range, it distorts the spectra and due to this the fittings are performed discarding the points of frequencies higher than that of the discontinuity.

## 3. RESULTS AND DISCUSSION

### 3.1. The equivalent circuit

To obtain all the TE properties from the impedance data obtained in this work , the experimental spectra were fitted using the equivalent circuit corresponding to a TE material sandwiched between two metallic contacts.[15] This equivalent circuit consists of an ohmic resistance $R_\Omega$ connected in series with the parallel combination of a constant temperature Warburg $Z_{WCT}$ and an adiabatic Warburg $Z_{Wa}$. Each of these elements are given by,

$$R_\Omega = \frac{\rho_{TE} L_{TE}}{A}, \tag{1}$$

$$Z_{WCT} = R_{TE}\left(\frac{j\omega}{\omega_{TE}}\right)^{-0.5} tanh\left[\left(\frac{j\omega}{\omega_{TE}}\right)^{0.5}\right], \tag{2}$$

$$Z_{Wa} = R_C\left(\frac{j\omega}{\omega_C}\right)^{-0.5} coth\left[\left(\frac{j\omega}{\omega_C}\right)^{0.5}\right], \tag{3}$$

where $\rho_{TE}$, $L_{TE}$, and $A$ are the electrical resistivity, length, and cross-sectional area of the TE material, respectively, $j^2$=-1, $\omega$ is the angular frequency, and $\omega_{TE}$ and $\omega_C$ are the characteristic angular frequencies of thermal diffusion in the TE sample ($\omega_{TE}=\alpha_{TE}/(L_{TE}/2)^2$; $\alpha_{TE}$ denoting the thermal diffusivity of the TE material) and in the contact ($\omega_C=\alpha_C/(L_C)^2$; $\alpha_C$ denoting the thermal diffusivity of the contact). $R_{TE}$ is the TE resistance,[27] and $R_C$ is a TE resistance induced by the contact. They are given by,

$$R_{TE} = \frac{S^2 T L_{TE}}{\lambda_{TE} A}, \tag{4}$$

$$R_C = 2\frac{S^2 T L_C}{\lambda_C A}, \tag{5}$$

where $\lambda_{TE}$ and $\lambda_C$ are the thermal conductivity of the TE material and the stainless steel contact, respectively, and $L_C$ the length of the latter.

From the curve fits, $R_\Omega$, $R_{TE}$, $R_C$, $\omega_{TE}$, and $\omega_C$ can be obtained. Hence, using Eq. (1), the electrical resistivity can be determined as,

$$\rho_{TE} = \frac{R_\Omega A}{L_{TE}}. \tag{6}$$

From Eq. (5), the Seebeck coefficient can be obtained as,

$$S = \sqrt{\frac{R_C \lambda_C A}{2TL_C}}. \tag{7}$$

It should be noted that in order to determine $S$ in Eq. (7), the thermal conductivity of the stainless steel contact is required, for which literature values may be used.[28] Combining Eq. (1) and Eq. (4),

$$zT = \frac{R_{TE}}{R_\Omega}. \tag{8}$$

### 3.2. Characterization by the impedance method

Five cycles were performed on the skutterudite sample, each cycle comprising a set of five impedance measurements at different temperatures (50, 100, 150, 200 and 250 ºC). Before the beginning of each cycle, the sample was newly assembled with fresh contacts. In order to obtain accurate impedance results, it is important to establish a suitable current amplitude for the measurements (the lowest amplitude possible with non-noisy measurements). This is to minimize the influence of non-linear effects such as the Joule heating and the variation of the TE properties with temperature, as discussed in our previous papers.[25,29] Hence, before performing the cycles, impedance spectroscopy measurements at different current amplitudes (40, 60, 80, 100 and 120 mA) were performed at each temperature in order to identify their optimal values. Fig. 2 shows the experimental impedance spectra and the corresponding fits for one of the five cycles measured. Fitting errors below 0.1, 0.5, and 12% were obtained for $R_\Omega$, $R_{TE}$, and $R_C$, respectively. It can be observed that even for the spectrum at 50 ºC, where the skutterudite shows lower performance and the impedance values are very small, the impedance response is clearly observed. In any case, the measured points differ in just few tenths of μΩ at high frequencies (bottom left part), and a powerful impedance analyzer (with high resolution and accuracy) is required in order to obtain sensitive measurements.

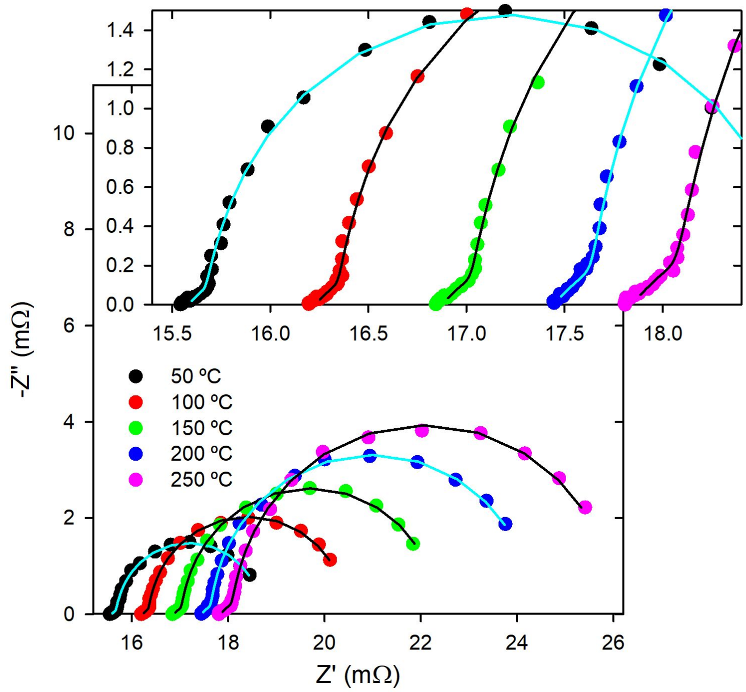


Fig. 2. Impedance spectroscopy measurements at different temperatures from one of the five measurement cycles performed. The dots represent the experimental values and the lines represent the fit to these data. The inset shows the magnification of the high frequency part.

The TE properties were obtained from Eq. (6) to Eq. (9) using the average values of $R_\Omega$, $R_{TE}$, and $R_C$ from the five measurements at each temperature. The thermal conductivity of the contact $\lambda_C$ (stainless steel AISI 304), which was needed for the Seebeck coefficient determination, was obtained from,[28]

$$\lambda_C = 10.33 + 15.4 \times 10^{-3} T - 7.0 \times 10^{-7} T^2. \tag{9}$$

The validity of Eq. (9) was verified by performing measurements of the stainless steel AISI 304 thermal conductivity by a laser flash apparatus (LFA 467 HT from Netzsch) up to 150 ºC. The deviations found with respect to the equation were lower than 2.7%. It is important in order to clearly discern the 45º straight line feature at high frequencies (see bottom part of the inset of Fig. 2) that $\lambda_C$ is around an order of magnitude higher than $\lambda_{TE}$, otherwise this feature will overlap with the semicircle part.

Fig. 3 shows the TE properties obtained by the impedance spectroscopy method compared with results from commercial equipment. All the properties show a good agreement with the commercial equipment measurements, except the electrical resistivity [Fig. 3(a)], which shows slightly higher values (around 6%), which is due to the contribution from the contact resistance, which is not completely suppressed since the W wires are inserted at the junctions. It is known that GaInSn liquid metal can have nm-length native oxide layers at its surface, which can impact its wetting behavior and electrical resistivity. This might contribute to the higher electrical resistivity values found.[30] It can be also observed for this property that as the temperature increases the error bars become larger and the trend slightly deviates from the behavior found with the commercial equipment. This is related to the fact that the GaInSn liquid metal tends to react with the TE sample at around 250 ºC. This is the limiting constraint on the maximum temperature of operation, since the rest of the elements of the setup can stand far higher temperature values. Hence, if a suitable solder or liquid metal for the sample to be measured were found, this method could increase its capability at higher temperatures. These aspects mentioned for the electrical resistivity also influence the $zT$ [Fig. 3(d)] due to Eq. (8), which exhibits larger errors and deviations at the highest temperatures.

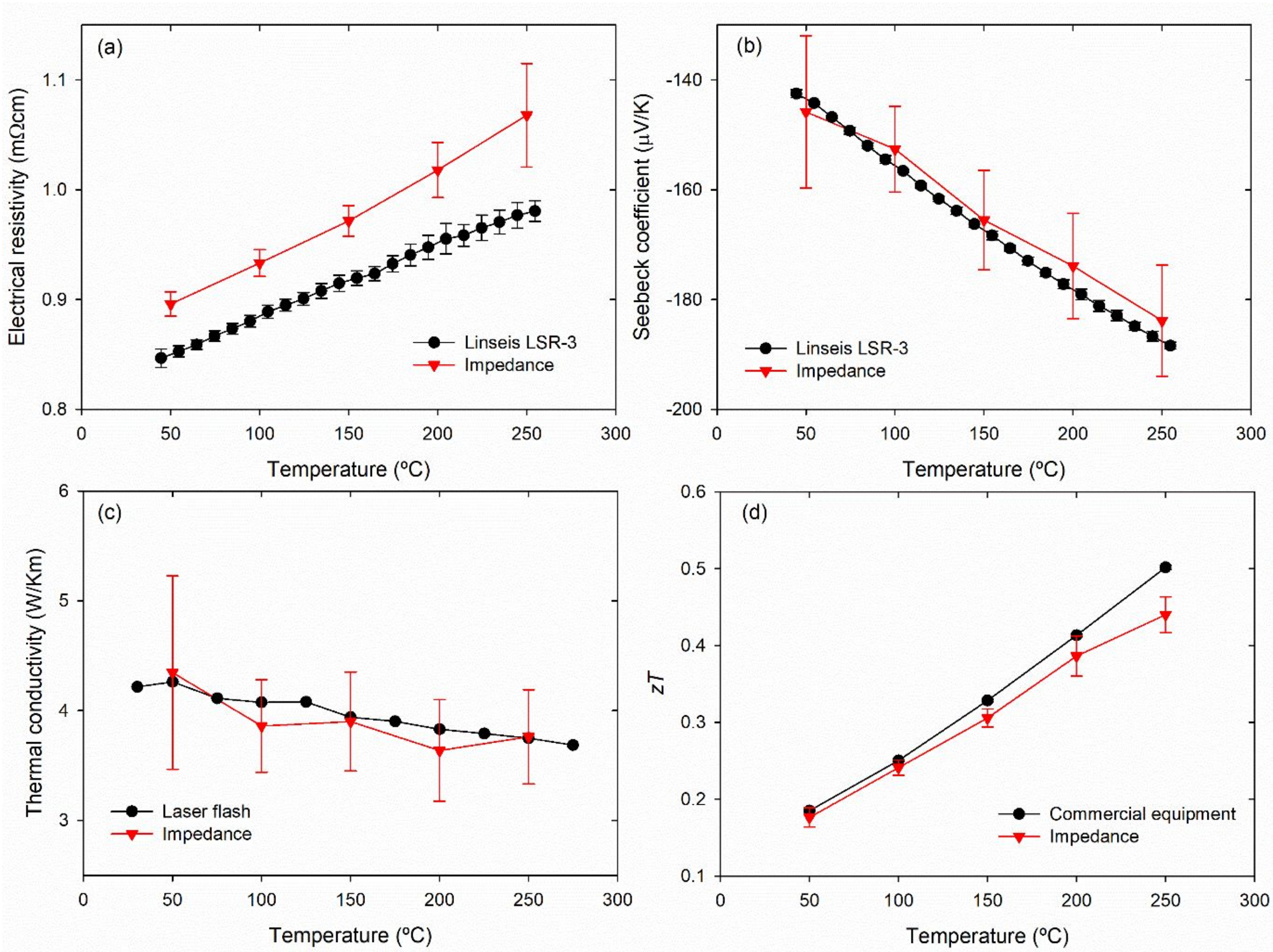


Fig. 3. (a) Electrical resistivity, (b) Seebeck coefficient, (c) thermal conductivity, and (d) zT values extracted from the impedance method and compared with results from different commercial equipment. The error bars account for the total combined random errors ($u_c$), excluding the contribution from the specific heat for the laser flash case. The confidence interval is 1$\sigma$.

### 3.3. Precision and accuracy evaluation

In order to quantify the precision and accuracy of the impedance method, random and systematic errors, respectively, were calculated for all the determined TE properties. The total combined random errors $u_c$ of each property were obtained using,[31]

$$u_c^2 = \sum_{i=1}^{N} \left(\frac{\partial f}{\partial x_i}\right)^2 u^2(x_i), \quad (10)$$

being $f$ each of the TE properties ($S$, $\lambda_{TE}$, $\rho_{TE}$, or $zT$), and $x_i$ each of the parameters with an associated error $u$. The random errors for the Seebeck coefficient were calculated taking into account (i) the standard deviation of the five measurements at each temperature to obtain the average value of $R_C$, (ii) the mean fitting error of the five $R_C$ measurements at each temperature, (iii) the uncertainty in the area of the sample, (iv) the uncertainty of the thermocouple ($u(T)$=1 ºC), and (v) the uncertainty in the length of the contacts, which was measured using a caliper ($u(L_C)$=0.005 mm). The contribution of the thermal conductivity of the contact was neglected. From all the above contributions, (i) and (ii) were the most significant compared to the others, which can be considered negligible.

The random errors for the thermal conductivity were calculated taking into account (i) the uncertainty of the Seebeck coefficient ($u_c(S)$), (ii) the uncertainty of the thermocouple ($u(T)$=1 ºC), (iii) the uncertainty in the length of the sample ($u(L_{TE})$=0.005 mm), (iv) the uncertainty in the area of the sample, and (v) the standard deviation of the five measurements at each temperature to obtain the average value of $R_{TE}$. The contribution from the fitting errors in $R_{TE}$ (which were <0.5%) was discarded since it was negligible in comparison with the standard deviation. From all the contributions considered, the uncertainty in the Seebeck coefficient and the standard deviation of $R_{TE}$ are the most significant, the Seebeck contribution being an order of magnitude higher. Hence, the precision in the thermal conductivity determination is strongly influenced by the precision in the Seebeck coefficient measurement.

The random errors for the electrical resistivity were calculated taking into account (i) the uncertainty in the length of the sample, (ii) the uncertainty in the cross-sectional area, and (iii) the standard deviation from the five measurements at each temperature to obtain the average $R_\Omega$. It should be noticed that the latter contribution is the most significant, since it is around two orders of magnitude larger than the others. As occurred for $R_{TE}$, the contribution of the fitting errors for $R_\Omega$ (<0.1%) was neglected. Finally, the random errors for $zT$ were calculated from the contributions of the standard deviations of both $R_\Omega$ and $R_{TE}$. The error bars shown in Fig. 3 correspond to the calculated random errors for each property, which are also shown in Table 1. Most of the random errors are ≈5.5%, <13%, <2.5%, and between 4 and 7% for $S$, $\lambda_{TE}$, $\rho_{TE}$, and $zT$, respectively, which demonstrates the good precision of the method, although the thermal conductivity is less precise due to the quadratic dependence on the Seebeck coefficient [see Eq. (7)]. At 50 ºC higher values are found for $S$ and $\lambda_{TE}$ due to a lower degree of repeatability at this temperature in one of the 5 cycles performed.

Table 1. Average values with their associated random, systematic and total errors of the thermoelectric properties of the skutterudite sample obtained by the impedance spectroscopy method.

| | **Temperature (ºC)** | **Mean value** | **Systematic error (%)** | **Random error (%)** | **Total error (%)** |
|---|---|---|---|---|---|
| Seebeck coefficient (*S*) | 50 | -145.8 μVK$^{-1}$ | 1.08 | 9.51 | 9.57 |
| | 100 | -152.6 μVK$^{-1}$ | 1.89 | 5.11 | 5.45 |
| | 150 | -165.5 μVK$^{-1}$ | 1.13 | 5.48 | 5.60 |
| | 200 | -173.9 μVK$^{-1}$ | 2.34 | 5.51 | 5.99 |
| | 250 | -183.9 μVK$^{-1}$ | 2.03 | 5.51 | 5.87 |
| Thermal conductivity ($\lambda_{TE}$) | 50 | 4.35 WK$^{-1}$m$^{-1}$ | 2.00 | 20.26 | 20.36 |
| | 100 | 3.86 WK$^{-1}$m$^{-1}$ | 5.28 | 10.93 | 12.14 |
| | 150 | 3.90 WK$^{-1}$m$^{-1}$ | 0.99 | 11.54 | 11.58 |
| | 200 | 3.64 WK$^{-1}$m$^{-1}$ | 5.05 | 12.71 | 13.68 |
| | 250 | 3.76 WK$^{-1}$m$^{-1}$ | 0.34 | 11.40 | 11.41 |
| Electrical resistivity ($\rho_{TE}$) | 50 | 0.896 mΩcm | 5.06 | 1.24 | 5.21 |
| | 100 | 0.933 mΩcm | 5.53 | 1.31 | 5.68 |
| | 150 | 0.972 mΩcm | 6.07 | 1.43 | 6.24 |
| | 200 | 1.018 mΩcm | 7.43 | 2.47 | 7.83 |
| | 250 | 1.068 mΩcm | 9.06 | 4.41 | 10.08 |
| Dimensionless figure of merit (*zT*) | 50 | 0.176 | 6.69 | 7.07 | 9.73 |
| | 100 | 0.241 | 0.04 | 4.07 | 4.07 |
| | 150 | 0.306 | 4.78 | 3.85 | 6.13 |
| | 200 | 0.386 | 1.97 | 6.77 | 7.05 |
| | 250 | 0.440 | 8.62 | 5.29 | 10.12 |

Systematic errors $u_s$ were calculated for the TE properties considering as true values the results obtained from the commercial equipment. They are also included in Table 1. Systematic errors are <2.5%, <5.5%, between 5 and 9%, and <9% for the *S*, $\lambda_{TE}$, $\rho_{TE}$, and *zT*, respectively, demonstrating a good agreement with the characterization performed with commercial equipment.

Finally, the total uncertainty of the method $u_T$ is obtained for each property as $u_T=(u_c^2+u_s^2)^{0.5}$ and also shown in Table 1. For *S* and $\lambda_{TE}$ the total errors are predominantly <6% and <14%, respectively. For these two parameters, it is evident that the principal contribution to the total error comes from the random error, which is higher than the systematic contribution. For $\rho_{TE}$ and *zT*, total errors are approximately from 5 to 10%, and from 4 to 10%, respectively. In this case the random and systematic contributions do not show the large differences as in the case of *S* and $\lambda_{TE}$ and more equally contribute to the total error.

## 4. CONCLUSIONS

In summary, the ability to perform a complete characterization of all TE properties of a bulk material as a function of temperature, from a single electrical impedance spectroscopy measurement, using one apparatus is demonstrated for a low-performance TE material (skutterudite sample) of modest properties up to 250 ºC. The TE properties were determined from fittings performed to the experimental impedance spectra employing a suitable equivalent circuit. Random errors were calculated by performing five measurements at each temperature remaking contacts, showing a good precision of the method (≈5.5%, <13%, <2.5%, and between 4 and 7% for the $S$, $\lambda_{TE}$, $\rho_{TE}$, and $zT$, respectively). The random errors in the determination of thermal conductivity are higher due to the quadratic dependence of this property with the Seebeck coefficient. Systematic errors were also calculated by comparison with characterization results from commercial equipment obtained from the same sample, resulting in errors <2.5%, <5.5%, between 5 and 9%, and <9% for the $S$, $\lambda_{TE}$, $\rho_{TE}$, and $zT$, respectively, which illustrates the accuracy of the method. These results demonstrate the potential of the method as a powerful tool to significantly facilitate the task of characterization of bulk TE materials and thus the search for a more efficient heat to electricity energy conversion.

## ACKNOWLEDGMENTS

BBP and JGC acknowledge financial support from the Spanish Agencia Estatal de Investigación under the Ramón y Cajal program (RYC-2013-13970), from the Generalitat Valenciana and the European Social Fund under the ACIF program (ACIF/2018/233), from the Universitat Jaume I under the project UJI-A2016-08, and the technical support of Raquel Oliver Valls and José Ortega Herreros. AVP and JPG wish to thank the UK Engineering and Physical Sciences Research Council (EP/K019767/1) for financial support.

## REFERENCES

(1) Fan, Z.; Ho, J. C.; Huang, B. Chapter 11. One-Dimensional Nanostructures for Energy Harvesting. In *One-Dimensional Nanostructures: Principles and Applications*; John Wiley & Sons, Inc.: Hoboken, NJ, USA, 2013; pp 237–270. https://doi.org/10.1002/9781118310342.ch11.

(2) Patowary, R.; Baruah, D. C. Thermoelectric Conversion of Waste Heat from IC Engine-Driven Vehicles: A Review of Its Application, Issues, and Solutions. *Int. J. Energy Res.* **2018**, *42*, 2595–2614.

https://doi.org/10.1002/er.4021.

(3) Champier, D. Thermoelectric Generators: A Review of Applications. *Energy Convers. Manag.* **2017**, *140*, 167–181. https://doi.org/10.1016/j.enconman.2017.02.070.

(4) Siddique, A. R. M.; Mahmud, S.; Heyst, B. Van. A Review of the State of the Science on Wearable Thermoelectric Power Generators (TEGs) and Their Existing Challenges. *Renew. Sustain. Energy Rev.* **2017**, *73*, 730–744. https://doi.org/10.1016/j.rser.2017.01.177.

(5) Snyder, G. J.; Toberer, E. S. Complex Thermoelectric Materials. *Nat. Mater.* **2008**, *7* (2), 105–114.

(6) Borup, K. A.; de Boor, J.; Wang, H.; Drymiotis, F.; Gascoin, F.; Shi, X.; Chen, L.; Fedorov, M. I.; Müller, E.; Iversen, B. B.; et al. Measuring Thermoelectric Transport Properties of Materials. *Energy Environ. Sci.* **2015**, *8* (2), 423–435. https://doi.org/10.1039/C4EE01320D.

(7) Stöhrer, U. Measurement of the Transport Properties of FeSi2 and HMS by Utilization of the Peltier Effect in the Temperature Range 50-800 $^{o}$C. *Meas. Sci. Technol.* **1994**, *5*, 440–446.

(8) de Boor, J.; Schmidt, V. Complete Characterization of Thermoelectric Materials by a Combined van Der Pauw Approach. *Adv. Mater.* **2010**, *22* (38), 4303. https://doi.org/10.1002/adma.201001654.

(9) Kallaher, R. L.; Latham, C. A.; Sharifi, F. An Apparatus for Concurrent Measurement of Thermoelectric Material Parameters. *Rev. Sci. Instrum.* **2013**, *84*, 013907. https://doi.org/10.1063/1.4789311.

(10) Kolb, H.; Dasgupta, T.; Zabrocki, K.; Mueller, E.; De Boor, J. Simultaneous Measurement of All Thermoelectric Properties of Bulk Materials in the Temperature Range 300-600 K. *Rev. Sci. Instrum.* **2015**, *86*, 073901. https://doi.org/10.1063/1.4926404.

(11) Vasilevskiy, D.; Simard, J. M.; Masut, R. A.; Turenne, S. System for Simultaneous Harman-Based Measurement of All Thermoelectric Properties, from 240 to 720 K, by Use of a Novel Calibration Procedure. *J. Electron. Mater.* **2015**, *44* (6), 1733–1742. https://doi.org/10.1007/s11664-014-3531-5.

(12) Martin, J.; Wong-Ng, W.; Green, M. L. Seebeck Coefficient Metrology: Do Contemporary Protocols Measure Up? *J. Electron. Mater.* **2015**, *44* (6), 1998–2006. https://doi.org/10.1007/s11664-015-3640-9.

(13) Dilhaire, S.; Patino-Lopez, L. D.; Grauby, S.; Rampnoux, J. M.; Jorez, S.; Claeys, W.; Ieee. Determination of ZT of PN Thermoelectric Couples by AC Electrical Measurement. In *XXI International Conference on Thermoelectrics, Proceedings ICT '02*; IEEE: New York, 2002; pp 321–324.

https://doi.org/10.1109/ict.2002.1190330.

(14) Downey, A. D.; Hogan, T. P.; Cook, B. Characterization of Thermoelectric Elements and Devices by Impedance Spectroscopy. *Rev. Sci. Instrum.* **2007**, *78* (9), 93904. https://doi.org/10.1063/1.2775432.

(15) García-Cañadas, J.; Min, G. Impedance Spectroscopy Models for the Complete Characterization of Thermoelectric Materials. *J. Appl. Phys.* **2014**, *116*, 174510. https://doi.org/10.1063/1.4901213.

(16) Yoo, C.-Y.; Kim, Y.; Hwang, J.; Yoon, H.; Cho, B. J.; Min, G.; Park, S. H. Impedance Spectroscopy for Assessment of Thermoelectric Module Properties under a Practical Operating Temperature. *Energy* **2017**, *152*, 834–839. https://doi.org/10.1016/j.energy.2017.12.014.

(17) Mesalam, R.; Williams, H. R.; Ambrosi, R. M.; García-Cañadas, J.; Stephenson, K. Towards a Comprehensive Model for Characterising and Assessing Thermoelectric Modules by Impedance Spectroscopy. *Appl. Energy* **2018**, *226*, 1208–1218. https://doi.org/10.1016/j.apenergy.2018.05.041.

(18) Thiébaut, E.; Pesty, F.; Goupil, C.; Guegan, G.; Lecoeur, P. Non-Linear Impedance Spectroscopy for Complete Thermoelectric Characterization: Beyond the ZT Estimation. *J. Appl. Phys.* **2018**, *124* (23), 235106. https://doi.org/10.1063/1.5063419.

(19) Fabregat-Santiago, F.; Garcia-Belmonte, G.; Mora-Sero, I.; Bisquert, J. Characterization of Nanostructured Hybrid and Organic Solar Cells by Impedance Spectroscopy. *Phys. Chem. Chem. Phys.* **2011**, *13* (20), 9083–9118. https://doi.org/10.1039/c0cp02249g.

(20) Mora-Sero, I.; Garcia-Belmonte, G. A.; Boix, P. P.; Vazquez, M. A.; Bisquert, J. Impedance Spectroscopy Characterisation of Highly Efficient Silicon Solar Cells under Different Light Illumination Intensities. *Energy Environ. Sci.* **2009**, *2* (6), 678–686. https://doi.org/10.1039/b812468j.

(21) Yuan, X. Z.; Wang, H. J.; Sun, J. C.; Zhang, J. J. AC Impedance Technique in PEM Fuel Cell Diagnosis - A Review. *Int. J. Hydrogen Energy* **2007**, *32* (17), 4365–4380. https://doi.org/10.1016/j.ijhydene.2007.05.036.

(22) Kotz, R.; Hahn, M.; Gallay, R. Temperature Behavior and Impedance Fundamentals of Supercapacitors. *J. Power Sources* **2006**, *154* (2), 550–555. https://doi.org/10.1016/j.jpowsour.2005.10.048.

(23) Walter, G. W. A Review of Impedance Plot Methods Used for Corrosion Performance Analysis of Painted Metals. *Corros. Sci.* **1986**, *26* (9), 681–703. https://doi.org/10.1016/0010-938x(86)90033-8.

(24) Irvine, J. T. S.; Sinclair, D. C.; West, A. R. Electroceramics: Characterization by Impedance Spectroscopy. *Adv. Mater.* **1990**, *2* (3), 132–138. https://doi.org/10.1002/adma.19900020304.

(25) Beltrán-Pitarch, B.; Prado-Gonjal, J.; Powell, A. V.; Ziolkowski, P.; García-Cañadas, J. Thermal Conductivity, Electrical Resistivity, and Dimensionless Figure of Merit (ZT) Determination of Thermoelectric Materials by Impedance Spectroscopy up to 250 °C. *J. Appl. Phys.* **2018**, *124* (2), 025105. https://doi.org/10.1063/1.5036937.

(26) Prado-Gonjal, J.; Phillips, M.; Vaqueiro, P.; Min, G.; Powell, A. V. Skutterudite Thermoelectric Modules with High Volume-Power-Density: Scalability and Reproducibility. *ACS Appl. Energy Mater.* **2018**, *1*, 6609–6618. https://doi.org/10.1021/acsaem.8b01548.

(27) García-Cañadas, J.; Min, G. Low Frequency Impedance Spectroscopy Analysis of Thermoelectric Modules. *J. Electron. Mater.* **2014**, *43* (6), 2411–2414. https://doi.org/10.1007/s11664-014-3095-4.

(28) Valencia, J. J.; Quested, P. N. Thermophysical Properties. In *ASM Handbook*; 2008; Vol. 15, pp 468–481. https://doi.org/10.1361/asmhba0005240.

(29) Beltrán-Pitarch, B.; Prado-Gonjal, J.; Powell, A. V.; García-Cañadas, J. Experimental Conditions Required for Accurate Measurements of Electrical Resistivity, Thermal Conductivity, and Dimensionless Figure of Merit (ZT) Using Harman and Impedance Spectroscopy Methods. *J. Appl. Phys.* **2019**, *125*, 025111. https://doi.org/10.1063/1.5077071.

(30) Khondoker, M. A. H.; Sameoto, D. Fabrication Methods and Applications of Microstructured Gallium Based Liquid Metal Alloys. *Smart Mater. Struct.* **2016**, *25* (9), 093001. https://doi.org/10.1088/0964-1726/25/9/093001.

(31) Evaluation of Measurement Data-Guide to the Expression of Uncertainty in Measurement. **1995**.

TOC Graphic

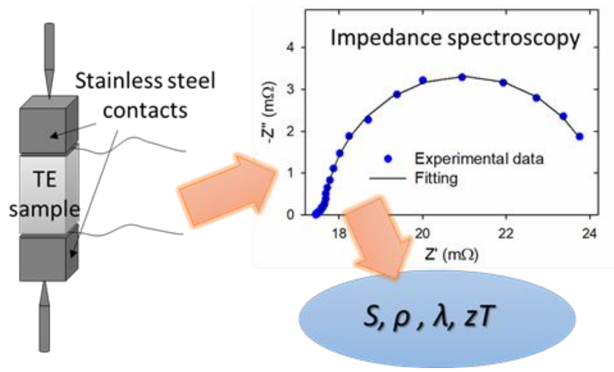
Stainless steel contacts
TE sample
Impedance spectroscopy
Experimental data
Fitting
-Z'' (mΩ)
Z' (mΩ)
S, ρ , λ, zT

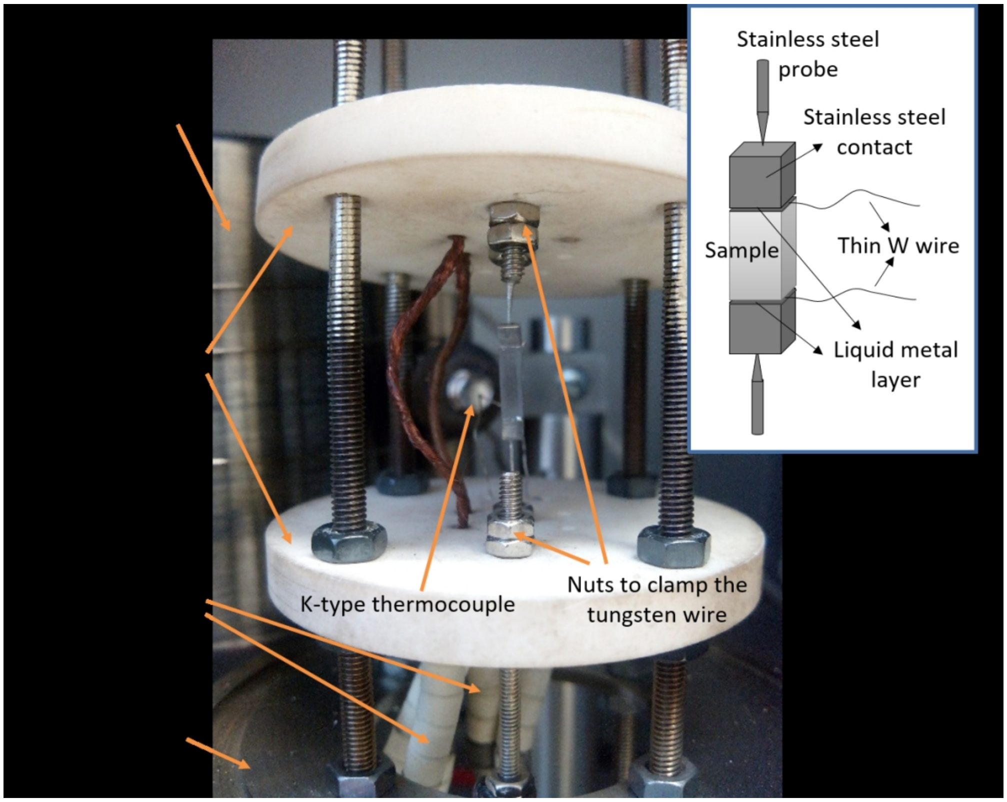


225x179mm (150 x 150 DPI)

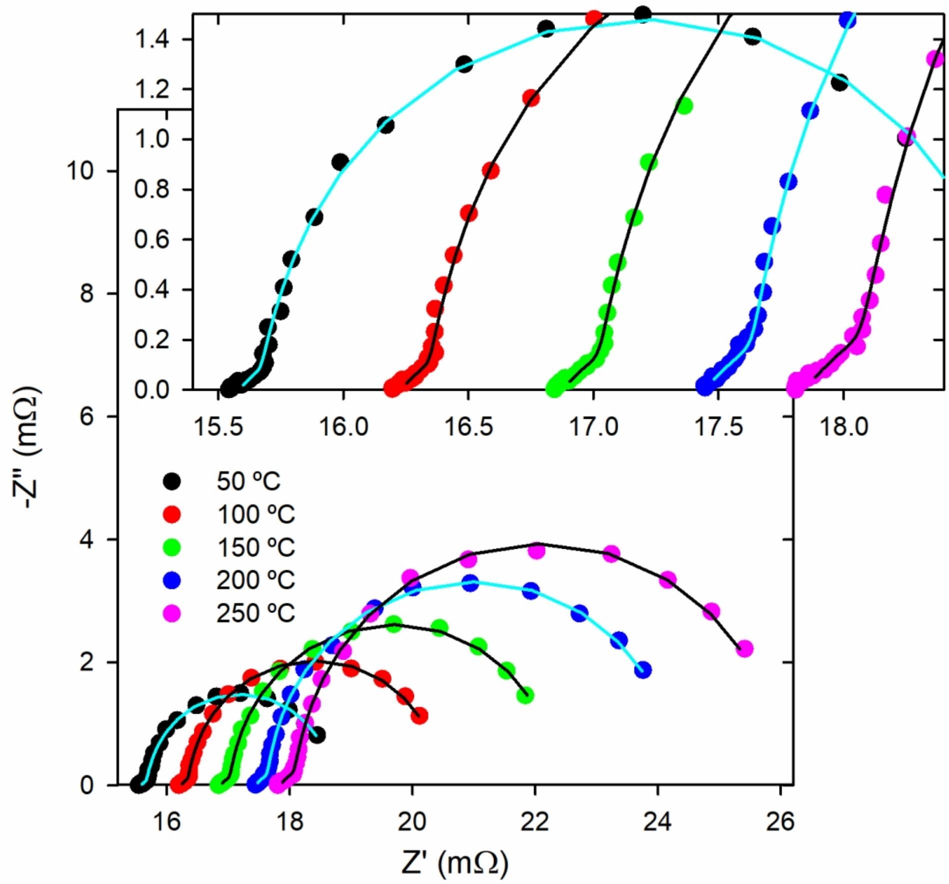


133x129mm (300 x 300 DPI)

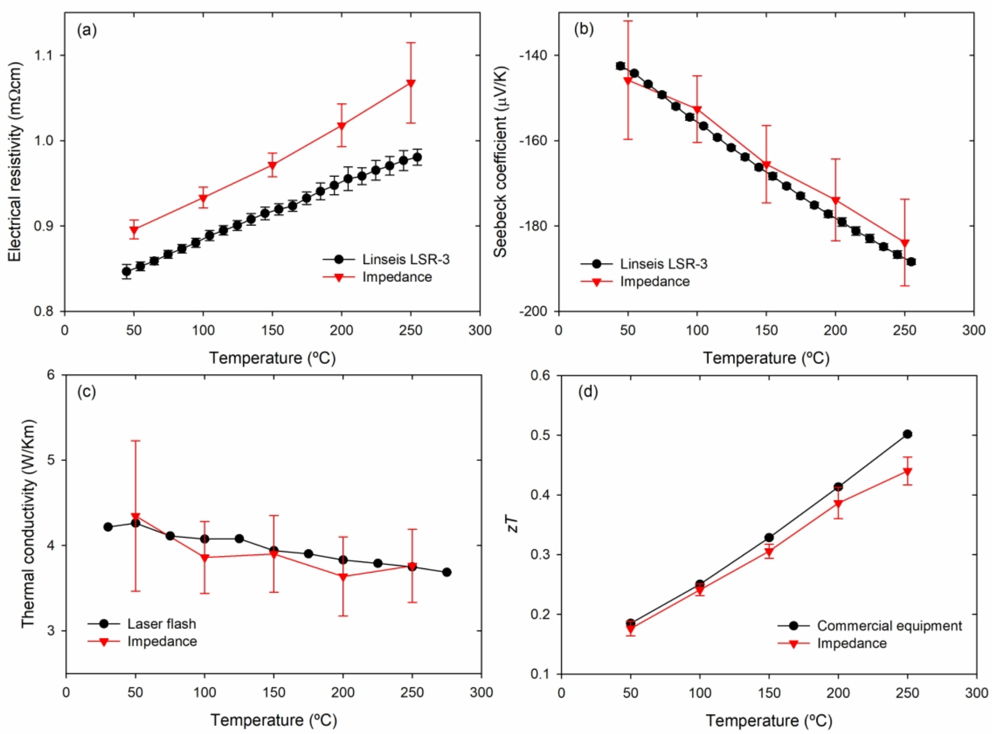


300x230mm (300 x 300 DPI)